Carboxyl-modified lignocellulose biomass of *Moringa oleifera* pod husk for effective removal of cationic dyes in single and binary dye systems

Khoiria Nur Atika Putri, Watchanida Chinpa*

*Division of Physical Science, Faculty of Science, Prince of Songkla University, Hat Yai, Songkhla 90110, Thailand,
watchanida.c@psu.ac.th (W. Chinpa)*

ABSTRACT

Value was added to an agricultural waste of *Moringa oleifera* pod husk (MOPH) by modifying the biomass with maleic anhydride (MA) to produce a cellulose-based adsorbent (MA-MOPH) that could remove crystal violet (CV) and methylene blue (MB) in single and binary dye systems. The biosorbent was characterized by Fourier-transform infrared spectroscopy, X-ray diffractometry, and thermogravimetric analysis. In single dye systems, the adsorption capacities of MA-MOPH were 378.50 mg g^{-1} for CV and 545.36 mg g^{-1} for MB. These values were obtained at 25°C, in solution at pH 8, at 180 and 60 min for CV and MB, respectively. The adsorption capacity of MA-MOPH for CV and MB was lower in the binary system due to competition between the two dyes. However, its adsorption capacity was higher than other adsorbents used to extract CV and MB in single dye systems. Overall, the adsorption process was well explained by the pseudo-second-order kinetics model and Langmuir isotherm model. MA-MOPH retained a satisfactory adsorption capacity in a repetitive adsorption process using the acetic acid solution as the desorbing agent. Therefore, MA-MOPH could be used as an economical biosorbent for the simultaneous removal of cationic dyes in water.

Keywords: Lignocellulosic biomass; Cationic dyes; Binary dye system; Adsorption

1. Introduction

The cradle-to-cradle concept is currently being adopted to overcome global pollution issues. This concept proposes the application or modification of waste materials to achieve an unlimited reuse that completely eliminates waste altogether [1]. In various economic sectors, the application of this concept could turn waste materials into valuable products or resources for further processes. The agricultural sector, for example, produces large amounts of crop residues that are currently waste materials. If the cradle-to-cradle concept were employed, crop residues could undergo modification to develop new products that would reduce the waste produced.

Moringa oleifera (MO) is a versatile plant widely cultivated in tropical countries, including India, Sri Lanka, Thailand, Malaysia and Philippines [2]. Its leaves, pods and seeds contain a variety of essential phytochemicals that are nutritionally and medically useful [3]. Oil is extracted from the seeds and afterwards the *Moringa oleifera* pod husk (MOPH) is discarded. However, MOPH has been developed as a composite reinforcement material [4] and a biosorbent to eliminate pollutants such as norfloxacin [5] and crystal violet (CV) [6]. As an alternative biosorbent material MOPH is cheap, renewable, and eco-friendly.

MOPH is lignocellulosic biomass mainly composed of cellulose. It is very versatile and can be modified to increase its adsorption efficiency. Cellulose possesses numerous hydroxyl groups which could readily bind with cationic

---

* Corresponding author.

pollutants via hydrogen bonding, ion–dipole forces, or electrostatic interaction [7–9]. Many studies have reported that the adsorption capacity of cellulose-based biosorbents increased after chemical modification [10–18]. Among the modification methods used to increase the adsorption capacity of cellulose-based materials, the introduction of carboxyl groups into the structure was effective because, once deprotonated, these functional groups exhibited excellent cation binding [18].

Maleic anhydride (MA) is a reagent used in cellulose-based esterification and has been reported to enhance the adsorption capacity of biosorbents toward cationic dyes [10,12–15,18]. Using commercially sourced cellulose modified with MA, Zhou et al. [13] prepared a biosorbent with an adsorption capacity of 370 mg g^{-1} toward malachite green. Qiao et al. [14] reported that a carboxylate-functionalized cellulose nanocrystal, derived from cellulose (99.5%) modified with MA, showed an adsorption capacity toward crystal violet (CV) of 243.9 mg g^{-1}. More recently, three highly effective adsorbents were prepared from corn stalk (CS), *Cinnamomum camphora* leaf (CCL), and *Cinnamomum camphora* sawdust (CCSD) with MA. Their adsorption capacities toward methylene blue (MB) were 870, 741, and 787 mg g^{-1}, respectively [18]. However, most previous works did not study a mixed dye solution that simulated industrial dye wastewater in the real world where the potential exists for competitive adsorption between dye ions. Therefore, the MA-modified MOPH presented in this study was used to remove CV and MB from water in single and binary systems. This work attempts to generate a high added-value product from agricultural waste. The MA-modified MOPH (MA-MOPH) biosorbent was studied using Fourier-transform infrared spectroscopy (FTIR), X-ray diffractometry (XRD), and thermogravimetric analysis (TGA) to determine chemical functionalities, structure and thermal stability, respectively. The effects of operating parameters, including pH, temperature, contact time, and initial concentration, were studied for both dyes. Adsorption kinetics and isotherms were investigated to describe MB and CV adsorption mechanisms in both the single and binary dye systems. The reusability of the cationic dye-loaded biosorbent was also investigated.

2. Materials and methods

2.1. Materials

MOPH was collected from Moringa trees cultivated in the southern region of Thailand. Maleic anhydride (MA) and dimethylacetamide (DMAc) were purchased from Fluka (Switzerland) and RCI Labscan (Thailand), respectively. Methylene blue (MB) (MW: 319.85 g mol^{-1}, APS Chemical, India) and crystal violet (CV) (MW: 407.98 g mol^{-1}, Loba Chemie, India) were used as adsorbates. Other analytical grade reagents such as sodium hydroxide (NaOH), hydrochloric acid (HCl), and acetone were supplied by RCI Labscan (Thailand).

2.2. Preparation of MA-MOPH

The pretreatment of MOPH and preparation of MOPH powder were carried out following the method described

by Keereerak and Chinpa [6]. The obtained MOPH powder was modified by chemical reaction using the method of Zhou et al. [13] with slight modification. MOPH and MA were mixed in the ratio of 1:10 and heated at 55°C for 20 min under continuous stirring. A volume of DMAc was added that had a mass five times the mass of MA. The mixture was reacted in a reflux system for 24 h at 150°C. MA-MOPH powder was obtained after washing the final product with DMAc, acetone and distilled water in that order. Lastly, the washed MA-MOPH was oven-dried and stored in a desiccator until further use.

2.3. Biosorbent characterization

The chemical functionalities of MOPH and MA-MOPH were investigated with the aid of FTIR (Equinox 55, Bruker, Germany) using the potassium bromide (KBr) pellet method. The spectrum produced by the sample-loaded KBr disks was analyzed from 4,000 to 400 cm^{-1}.

The crystallinity index (CrI) of the biosorbent was determined by X-ray diffractometer (X'Pert MPD, Philips, Netherlands) and the CrI value was calculated using the maximum intensity of the 002 lattice diffraction peak (I_{002}) and the scattered intensity of the amorphous part (I_{am}), according to the following equation [19]:

$$CrI\,(\%) = \left(\frac{I_{002} - I_{am}}{I_{002}}\right) \times 100 \tag{1}$$

TGA (TGA 7, PerkinElmer, USA) was employed to study the thermal degradation behavior of the biosorbent. Measurement was carried out under N$_2$ at 30°C to 900°C, ramping at 10°C min^{-1}.

The MA-MOPH point of zero charge (pH$_{PZC}$) was determined using the method described by Jia et al. [20]. The pH of the solution in contact with the biosorbent was varied from 2 to 10 and these values were recorded as pH$_i$. MA-MOPH was added to each solution and after 24 h, the pH values of the solutions were recorded as pH$_f$. The curve of pH$_f$ vs. pH$_i$ was plotted and the point at which pH$_f$ was equal to pH$_i$ was determined as the pH$_{PZC}$.

2.4. Adsorption study

The optimum condition for CV and MB adsorption on MA-MOPH was determined by varying the operating parameters of pH, temperature, contact time, and adsorbate initial concentration. The effects on adsorption were observed. pH was varied from 3–9, the temperature at 25°C, 35°C and 45°C, contact time from 5–360 min, and adsorbate initial concentration from 40–750 mg L^{-1}. In the single dye system, 20 mL CV or MB solution was adsorbed on 0.005 g of MA-MOPH under agitation at 60 rpm. All experiments were carried out in at least three replications. The residual dye concentration after adsorption was measured by a UV-Visible spectrometer (Lambda 25, PerkinElmer, USA). The concentration of residual dye after adsorption was used to calculate the adsorption capacity (q, mg g^{-1}) following Eq. (2):

$$q = \frac{(C_0 - C_t)V}{m} \tag{2}$$

where C_0, C_t and C_e (mg L^{-1}) were respectively the initial liquid-phase dye concentration, and the liquid-phase concentrations of dye at time t and equilibrium; V (mL) was the volume of the solution and m (g) was the weight of the biosorbent.

In the binary dye system, MB and CV were mixed at a volume ratio of 1:1 to obtain a total volume of 20 mL and initial concentrations were designated in the range of 40 to 750 mg L^{-1}. The dye mixture was adsorbed on 0.005 g of MA-MOPH powder and residual dye concentrations were determined by a UV-Visible spectrometer. This experiment was performed at 25°C and pH 8. To subtract the mutual interference of CV and MB in the binary solution, absorbance at 588 nm for CV and 666 nm MB was calculated according to the following equations [21,22]:

$$A_{588}^{Total} = A_{588}^{CV} + A_{588}^{MB} \tag{3}$$

$$A_{666}^{Total} = A_{666}^{CV} + A_{666}^{MB} \tag{4}$$

$$\frac{A_{666}^{CV}}{A_{588}^{CV}} = \frac{\varepsilon_{666}^{CV}}{\varepsilon_{588}^{CV}} = K_1 \tag{5}$$

$$\frac{A_{588}^{MB}}{A_{666}^{MB}} = \frac{\varepsilon_{588}^{MB}}{\varepsilon_{666}^{MB}} = K_2 \tag{6}$$

$$A_{588}^{CV} = \frac{A_{588}^{Total} - K_2 \cdot A_{666}^{Total}}{1 - K_1 \cdot K_2} \tag{7}$$

$$A_{666}^{MB} = \frac{A_{666}^{Total} - K_1 \cdot A_{588}^{Total}}{1 - K_1 \cdot K_2} \tag{8}$$

where the total absorbance of mixture solutions of CV and MB are denoted A_{588}^{Total} and A_{666}^{Total}, respectively; A_{588}^{CV}, A_{588}^{MB}, A_{666}^{CV}, and A_{666}^{MB} are the absorbance of CV and MB at 588 and 666 nm. The terms ε_{588}^{CV}, ε_{588}^{MB}, ε_{666}^{CV} and ε_{666}^{MB} are the coefficients of molar absorptivity of the dyes at both wavelengths. Meanwhile, K_1 and K_2 are the molar absorptivity coefficient ratios. Finally, the residual concentrations of CV and MB in the dye mixture were obtained from the values of A_{588}^{CV} and A_{666}^{MB} by using the standard curve method [21,22].

2.5. Biosorbent reusability

The MA-MOPH sorbent was assessed for its ability to repeatedly adsorb dye over a period of time. Firstly, 20 mL of MB or CV at an initial concentration of 70 mg L^{-1} at pH 8 were adsorbed on 0.005 g of MA-MOPH powder under agitation for the optimum contact time for each dye. The dye-loaded MA-MOPH powder was desorbed with 1.0 M acetic acid until the solution was colorless. The powder was then washed using distilled water and used again to adsorb the same concentration of dye. This procedure was repeated five times.

3. Results and discussion

3.1. Biosorbent characterization

The chemical functionalities of MA-MOPH were elucidated using FTIR. Unmodified MOPH (Fig. 1a) contained the native functional groups of lignocellulosic materials, including hydroxyl groups (-OH) at 3,418 cm^{-1}, carbonyl groups (–C=O) at 1,737 cm^{-1}, and ether groups (–C–O) assigned at 1,058 cm^{-1} [23,24]. The peak located at 1,640 cm^{-1} was attributed to adsorbed water [24]. A similar pattern was also observed for MA-MOPH. However, the strong peaks at 1,625 and 1,733 cm^{-1} were assigned to the vinyl (C=C) and carboxyl groups in the structure of MA [13]. Therefore, FTIR analysis confirmed that MOPH was successfully modified with MA.

The XRD patterns of MOPH and MA-MOPH (Fig. 1b) presented diffraction peaks at 2θ around 16.1°, 22.0°, and 34.7°, which are characteristics of the crystal lattice structure of cellulose type I [25]. However, MA-MOPH produced less intense peaks than unmodified MOPH. The crystallinity index decreased from 32% for MOPH to 21% for MA-MOPH. This finding indicated that modification with MA could alter the crystal structure of cellulose in MOPH [12,14]. A similar result was reported for the modification of cellulose and cellulose nanocrystals with MA [12,14].

The thermal degradation behavior of the MOPH-based biosorbent was studied using TGA. The thermogram of MA-MOPH and untreated MOPH indicated similar thermal degradation behaviors (Fig. 1c). In both thermograms, the initial degradation at ca. 38°C–120°C was related to the loss of moisture from the material. The loss of weight at 200°C–400°C was related to the decomposition of hemicellulose and cellulose. The degradation of lignin was observed at 200°C–700°C [26]. However, the initial thermal decomposition temperature of MA-MOPH was lower than that of MOPH and the thermal cleavage temperature around 300°C–400°C was higher than that of MOPH. Similar findings were reported for cellulose nanocrystals modified with MA and attributed to the abundant carboxyl groups obtained through modification with MA [14].

The pH$_{PZC}$ of MA-MOPH was 4.1 (Fig. 1d). Thus, it was hypothesized that, when the pH value is greater than pH$_{PZC}$, the charge on the surface of MA-MOPH is predominantly negative [27]. However, at pH values lower than pH$_{PZC}$, the surface of MA-MOPH was mainly positively charged. These findings helped later to explain the effect of solution pH on the dye adsorption capacity of the sorbent.

The adsorption of CV at an initial concentration of 70 mg g^{-1} on MA-MOPH was compared with adsorption on unmodified MOPH and the results (Fig. 2a) demonstrated that the efficiency of dye adsorption was significantly higher on MA-MOPH. The adsorption efficiency of MA-MOPH toward methyl red or direct yellow was also investigated. The biosorbent hardly adsorbed either dye (Fig. 2b). Since both are anionic dyes, this result could be attributed to the similarity between the molecular charges of MA-MOPH and the dyes, which induced electrostatic repulsion. MB and CV were then used as dye pollutant models for the adsorption study.
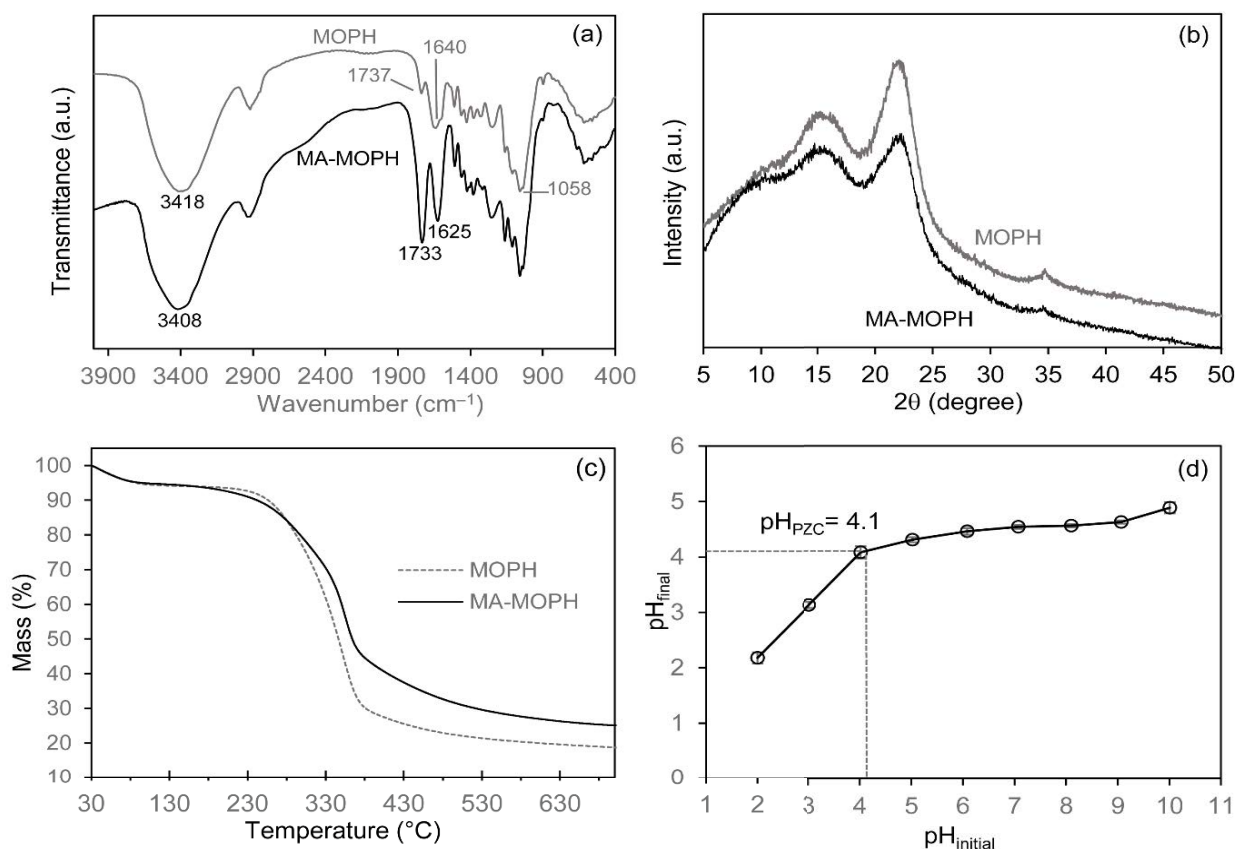
Fig. 1. FTIR spectra (a), XRD patterns (b), and TGA thermograms (c) of unmodified MOPH and MA-MOPH and the curve of pH_f vs. pH_i to determine pH_{PZC} (d).
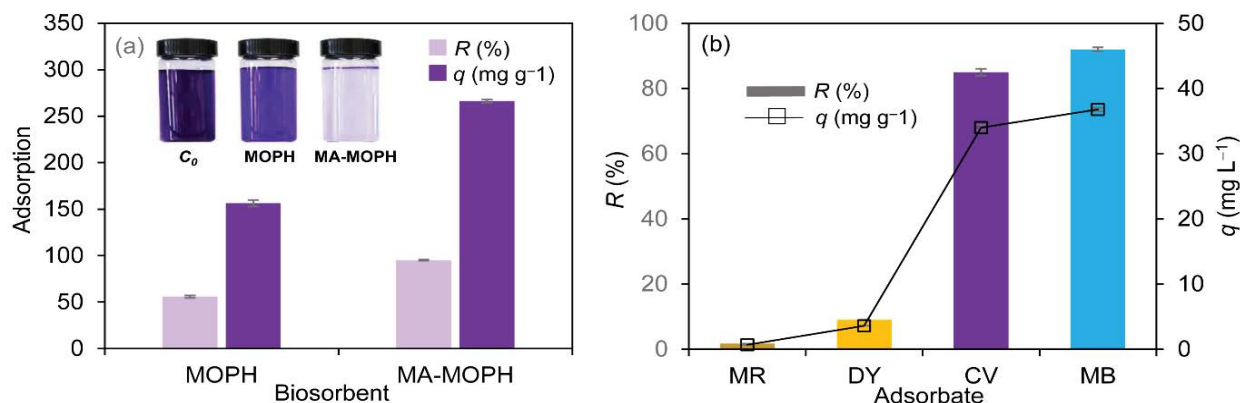

Fig. 2. Adsorption efficiency of MOPH and MA-MOPH toward CV at C_0 of 70 mg g^{-1} (a) and adsorption efficiency of MA-MOPH toward different dyes at C_0 of 10 mg g^{-1} (b) (Condition: at natural dye solution pH, 25°C and a contact time of 2 h).

3.2. Effect of pH on adsorption

MA-MOPH consisted of carboxyl and hydroxyl groups. The ionic properties of these two groups were influenced by the pH value of the solution system. In this study, the dye adsorption capacity (q) of MA-MOPH increased with increments of solution pH from pH 3 to 8 (Fig. 3a). The value of q was higher in the basic condition than in the acidic condition both for CV and for MB. At solution pH < pH_{PZC}

(pH_{PZC} = 4.1), the surface charge of MA-MOPH was presumed to be positive, in which condition the repulsion effect increased since the dye molecules were similarly charged. At solution pH > pH_{PZC}, the surface of MA-MOPH was negatively charged, which was a very favorable condition to generate electrostatic interaction with the positively charged CV and MB dye molecules [7]. However, the slight decrease in q values in the solution above pH 8 could be related to hydroxyl moieties that could compete with the negative
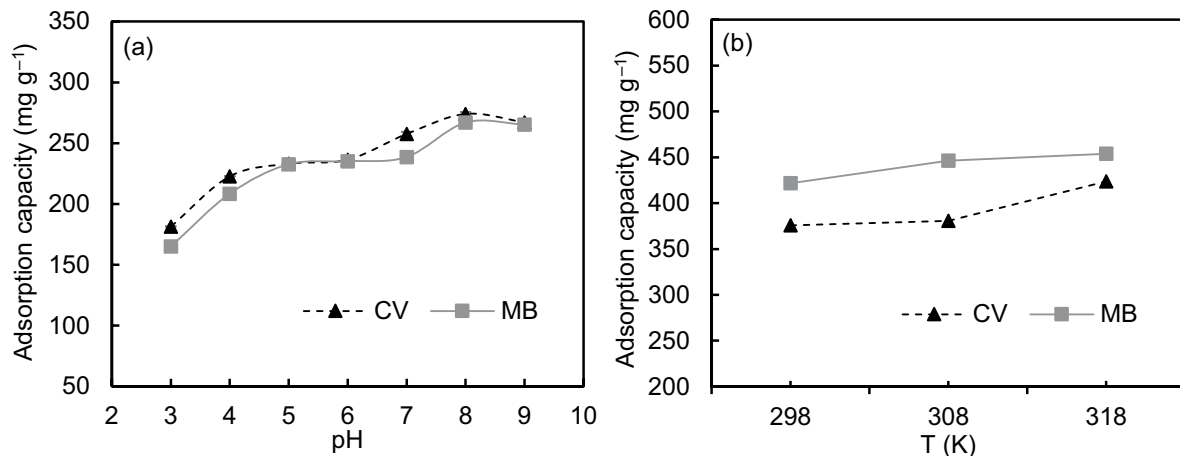
Fig. 3. Effects on adsorption capacity of MA-MOPH toward CV and MB of pH at 25°C and C_0 of 70 mg L^{-1} (a) and of temperature at pH 8 and C_0 of 150 mg L^{-1} (b).

charges of MA-MOPH to interact with dye molecules [28]. In light of these observations, a solution pH of 8 was chosen as the optimum operating parameter for the following studies of CV and MB adsorption on MA-MOPH.

3.3. Effect of temperature on adsorption and adsorption thermodynamics study

Changes in solution viscosity due to temperature is known to affect the diffusion rate of an adsorbate through the external boundary layer [29,30]. In this study, the adsorption capacity of MA-MOPH for CV and MB slightly increased with increases in temperature (Fig. 3b). This result implied that temperature had only a small effect on the adsorption capacity of MA-MOPH and, therefore, this biosorbent may be able to eliminate cationic dyes in a wide range of temperatures [29].

The adsorption of CV and MB on MA-MOPH at various temperatures was used to determine the thermodynamic behavior of the adsorption process in the single dye systems. The thermodynamic parameters of enthalpy ($\Delta H°$) and entropy ($\Delta S°$) were calculated from plots of $\ln K_c$ vs. $1/T$ based on Eq. (9) where Gibb's free energy ($\Delta G°$) was obtained from Eq. (10):

$$\ln K_c = \frac{\Delta S°}{R} - \frac{\Delta H°}{RT} \tag{9}$$

$$\Delta G° = -RT \ln K_c \tag{10}$$

where K_c is the ratio between the dye equilibrium concentrations in the solid phase and in the solution phase after adsorption, T is the absolute temperature (K) and R is an ideal gas constant of 8.314 J mol^{-1} K^{-1}. All calculated parameters are listed in Table 1.

The negative values of $\Delta G°$ indicated the spontaneity of CV and MB adsorption on MA-MOPH and the more negative values of $\Delta G°$ signified that temperature elevation was favorable for the adsorption reaction [31]. For both dyes, the magnitude of $\Delta H°$, which was positive, signified

Table 1
Thermodynamic parameters of CV and MB adsorption on MA-MOPH

Dye	Temperature (K)	$\Delta G°$ (kJ mol^{-1})	$\Delta H°$ (kJ mol^{-1})	$\Delta S°$ (J mol^{-1} K^{-1})
CV	298	−4.71	14.06	62.58
	308	−4.96		
	318	−5.98		
MB	298	−5.57	10.69	54.44
	308	−6.09		
	318	−6.66		

the endothermic nature of the adsorption processes. Other than that, the positive $\Delta S°$ values indicated the increased disorder of the solid–liquid interfaces during the adsorption processes [27]. Similar results were reported in the adsorption of CV and MB using N-maleyl chitosan cross-linked P(AA-co-VPA) hydrogel [31] and treated lemongrass leaf fiber [32], respectively.

3.4. Effect of contact time on adsorption

The optimal contact time for the adsorption of CV and MB on MA-MOPH in both single and binary dye systems was investigated from 5–360 min and determined by the adsorption capacity. The uptake of both dyes was rapid from 5–30 min and slowed down at 60 min (Fig. 4a and b). Faster CV and MB adsorption at the initial stage was related to the vacancy of MA-MOPH active sites which enabled easier binding of dye molecules onto the MA-MOPH surface at the beginning of the adsorption process. The rate of dye uptake slowed as time elapsed and finally reached equilibrium in the single systems at 180 min for CV and 60 min for MB. In the binary system, equilibrium was reached at 180 min for both dyes. These times were determined as the optimum contact times for adsorption of the respective dyes in each system. The saturation state occurred after active sites on the MA-MOPH biosorbent surface were
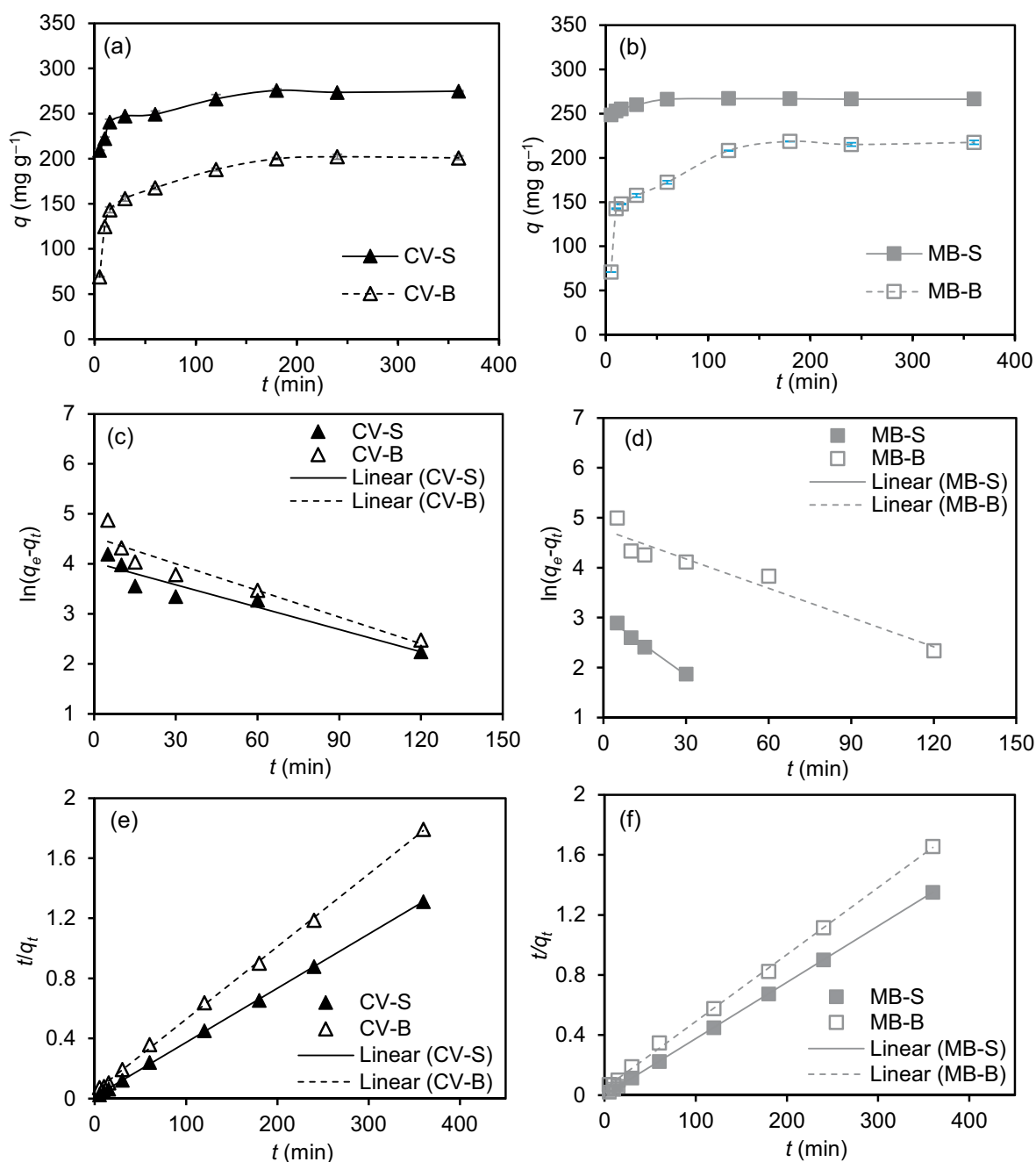
Fig. 4. Effect of contact time on adsorption capacity of MA-MOPH toward CV (a) and MB (b). The pseudo-first-order model fitted to the experimental data of CV (c) and MB (d) and the pseudo-second-order model fitted to the experimental data of CV (e) and MB (f). (Condition: C_0 of 70 mg L^{-1}, pH 8 at 25°C, S = Single system and B = Binary system).

occupied by adsorbed dye molecules. In the binary system, the overall adsorption capacity of CV and MB was considerably lower than it was in the single system. The disparity could be related to competition between MB and CV molecules for active sites of MA-MOPH in the binary system.

The possible mechanisms of MB and CV adsorption on MA-MOPH in the single and binary systems were studied by fitting with the pseudo-first-order and pseudo-second-order kinetics models. The adsorption kinetics models were fitted to experimental data collected at pH 8 and 25°C.

Pseudo-first-order and the pseudo-second-order equations are described in Eqs. (11) and (12) [33,34], respectively:

$$\ln\left(q_e - q_t\right) = \ln q_e - k_1 t \tag{11}$$

$$\frac{t}{q_t} = \frac{1}{k_2 q_e^2} + \frac{1}{q_e} t \tag{12}$$

where q_e is the dye concentration at adsorption equilibrium, q_t is the dye concentration at a specific time (t) and k_1 is the pseudo-first-order rate constant (min^{-1}) while k_2 is the pseudo-second-order constant (g mg^{-1} min^{-1}).

On the whole, the pseudo-second-order had the best fit for MB and CV adsorption processes in both the single and binary dye systems (Figs. 4c–f). The R^2 value from the pseudo-second-order, which was closest to 1 (Table 2), indicated that this model best represented the MB and CV adsorption mechanisms on MA-MOPH. Moreover, the calculated q_e values derived from the pseudo-second-order fitting were similar to the experimental q_e values (Table 2). Thus, it was concluded that the adsorption process was governed by the interaction between the opposite charges present on the cationic dyes and available functional groups of the biosorbent [35,36].

3.5. Effect of dye initial concentrations on adsorption

The adsorption of MB and CV on MA-MOPH in the single and binary dye systems was investigated as a function of concentration by varying dye initial concentration in a range of 40–750 mg L^{-1}. A high concentration of dye increased the driving force that transports dye molecules from the solution to the biosorbent surface [13]. In this study, adsorption capacity increased with increments of dye initial concentration from 40–200 mg L^{-1} (Fig. 5a). However, increases in the adsorption of MB and CV on MOPH were insignificant at initial concentrations higher than 200 mg L^{-1}. The limited amount of unoccupied active sites at high concentrations of dye caused saturation of the biosorbent, leading to an equilibrium state of adsorption. Furthermore, the q values were higher for MB than CV in both dye systems. The explanation for these results lies in the comparative sizes of the two dye molecules. The MB molecule is smaller than the CV molecule and therefore more easily adsorbed. The lower adsorption capacity of MA-MOPH toward both dyes in the binary system indicated the presence of competitive adsorption between CV and MB.

The adsorption equilibrium data of CV and MB on MA-MOPH in the single and binary systems were studied using isothermal models. Amongst all isotherm models, the Langmuir and Freundlich models are the most well-known and are widely applied to adsorption processes. The Langmuir model assumes the biosorbent active sites are homogeneous and the adsorbate adsorbs onto the adsorbent in a monolayer form without interaction between adsorbed molecules [27,37]. The Langmuir isotherm models are expressed by Eq. (13) [38].

$$\frac{C_e}{q_e} = \frac{C_e}{q_m} + \frac{1}{q_m K_L} \tag{13}$$

where C_e is adsorbate concentration in the equilibrium state (mg L^{-1}), q_e is adsorption capacity in the equilibrium state (mg g^{-1}), while K_L is Langmuir constant (L mg^{-1}) and q_m is maximum adsorption capacity of the biosorbent (mg g^{-1}).

The Freundlich model is commonly used to describe the adsorption on heterogeneous surface and multilayer adsorption on a sorbent surface where there is interaction between adsorbed molecules [37] and this model is expressed by Eq. (14) [39].

$$\ln q_e = \ln K_F + \frac{1}{n} \ln C_e \tag{14}$$

where K_F is the Freundlich adsorption constant ((mg g^{-1}) (L mg^{-1})$^{1/n}$) and n is the adsorption intensity.

The R^2 value yielded by fitting the Langmuir isotherm model to the experimental data was closer to 1 than the R^2 yielded by fitting the Freundlich isotherm model to the experimental data (Table 3 and Fig. 5b and c). Moreover, the values of q_m obtained from the Langmuir model (Table 3) were close to the values obtained from the experimental data. Therefore, the Langmuir isotherm could better describe the adsorption of MB and CV on MA-MOPH in both the single and binary systems. Table 4 shows the adsorption efficiency of MA-MOPH compared to other adsorbents. It could be seen that this biosorbent derived from biomass showed a high adsorption capacity for both CV and MB. The preparation procedure of the proposed required only two reagents: MA and DMAc. Moreover, after the separation of the MA-MOPH biosorbent, unreacted MA and DMAc could be recovered by distillation.

In the binary system, competition effects between ions of the two dyes could be deduced from studying the ratios of maximum adsorption capacity for the dye in the binary

Table 2
Kinetic parameters of CV and MB adsorption on MA-MOPH

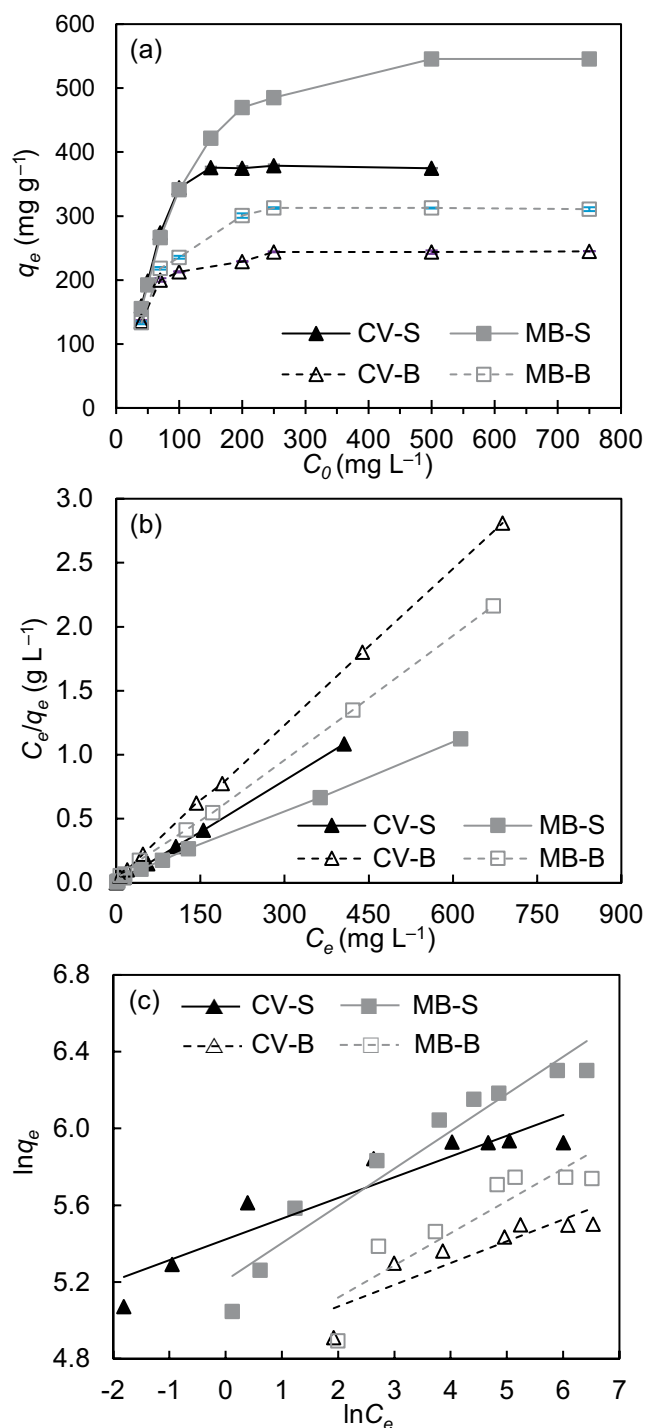| Model	Parameters	Single system		Binary system	
		CV	MB	CV	MB
Experimental					
q_e (mg g^{-1})	–	275.65	266.89	199.97	218.52
Pseudo-first-order	q_e (mg g^{-1})	56.13	20.79	93.52	116.76
	k_1 (min^{-1})	1.49×10^{-2}	3.95×10^{-2}	1.78×10^{-2}	1.96×10^{-2}
	R^2	0.9129	0.9892	0.9125	0.9299
Pseudo-second-order	q_e (mg g^{-1})	277.78	270.27	208.33	222.22
	k_2 (g mg^{-1} min^{-1})	1.09×10^{-3}	1.18×10^{-3}	5.18×10^{-4}	4.47×10^{-4}
	R^2	0.9998	0.9999	0.9994	0.9990

Fig. 5. Effect of initial concentration on adsorption capacity of MA-MOPH toward CV and MB (a): Langmuir (b) and Freundlich (c) isotherm models fitted to experimental data (Condition: pH 8 at 25°C, contact time of 180 and 60 min for CV and MB, respectively, S = Single system and B = Binary system).

Table 3
Results of adsorption isotherms for CV and MB adsorption on MA-MOPH

Models	Parameters	Single system		Binary system	
		CV	MB	CV	MB
Experimental					
q_m (mg g^{-1})	–	378.50	545.36	243.09	312.78
Langmuir	q_m (mg g^{-1})	370.37	555.56	250.00	312.50
	K_L (L mg^{-1})	1.59	0.11	0.15	0.13
	R^2	0.9999	0.9993	0.9999	0.9997
Freundlich	K_F ((mg g^{-1}) (L mg^{-1})$^{1/n}$)	226.26	182.75	127.27	119.40
	n	9.26	5.15	8.84	5.95
	R^2	0.8843	0.9344	0.7956	0.8008

adsorption was independent of the presence of other dyes: when $q_{mb}/q_{ms} > 1$, adsorption was promoted by the existence of other dyes in the mixture [44]. The values of q_{mb}/q_{ms} for MB and CV were less than one, suggesting that there was a competition between CV and MB molecules for active sites on the MA-MOPH biosorbent [44,45]. Since the molecular weight of MB is less than that of CV, MB was probably adsorbed first. The adsorption capacity of MA-MOPH in the binary system was higher than other adsorbents toward CV and MB in single systems reported in the literature (Table 4). MA-MOPH is an effective and low-cost biosorbent capable of simultaneously eliminating two cationic dyes in wastewater.

3.6. Biosorbent reusability

The reusability of the MA-MOPH biosorbent was evaluated by the repeated adsorption of CV and MB to determine any loss of technical efficiency that might increase cost in a scaled-up industrial application. The dye-loaded biosorbent was desorbed with 1.0 M CH$_3$COOH solution, which replaced the positive charges of the dyes with H$^+$ ions [46]. The regenerated MA-MOPH was able to maintain its adsorption capacity towards MB for 5 consecutive cycles with only a negligible reduction in adsorption (Fig. 6). CV adsorption on MA-MOPH, meanwhile, slightly decreased throughout the first to third cycle followed by a quite significant reduction that started at the fourth cycle and continued. This reduction was attributed to the incomplete desorption of CV by CH$_3$COOH [9].

3.7. Interaction between biosorbent and cationic dyes

The effects of desorption in an acidic medium, the study of solution pH that indicated optimal adsorption in basic solution (pH 8), and the results of the adsorption kinetics study, led to the conclusion that adsorption occurred through electrostatic interaction between positive charges of the dyes and negative charges on carboxylic and hydroxyl groups of MA-MOPH. Possible mechanisms of adsorption are proposed below [7]:

system (q_{mb}) to the maximum adsorption capacity for the same dye in the single system (q_{ms}) [44]. The ratios of both values described three competitive effects as follows: when $q_{mb}/q_{ms} < 1$, adsorption was suppressed by the existence of other dyes in the dye solution: when $q_{mb}/q_{ms} = 1$,

Table 4
Maximum adsorption capacity of various adsorbents from Langmuir isotherm model

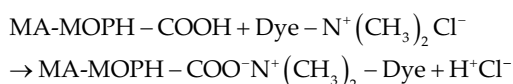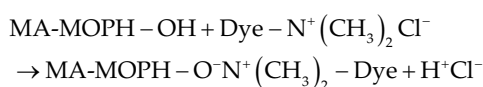| Adsorbent	Maximum adsorption capacity (q_m, mg g^{-1})			
	Single system		Binary system	
	CV	MB	CV	MB
Cellulose modified with maleic anhydride [12]	33.69	194.6	–	–
Carboxylate-functionalized cellulose nanocrystals [14]	243.9	–	–	–
Corn stalk fiber grafted poly(acrylic acid) [16]	–	354.1	–	–
M-CS, M-CCL, M-CCSD [18]	–	870, 741, 787	–	–
Crosslinking thiourea-modified sugarcane bagasse cellulose with carboxymethyl cellulose hydrogel [22]	574.7	632.9	427.4	555.6
Industrial microbial waste [29]	175.44	92.59	74.63	52.9
Cellulose-based modified citrus peels/calcium alginate composite [30]	881.56	923.07	884.11	795.14
Natural clay [40]	231.74	279.95	~160	~190
Sn (O, S) nanoparticles loaded on activated carbon [41]	115.3	109.2	103	95.7
Carboxymethyl cellulose hydrogels beads [42]	–	82	–	–
Carboxylate-modified lignosulfonate [43]	–	613.5	–	–
MA-MOPH (this study)	370.37	555.56	250.00	312.50
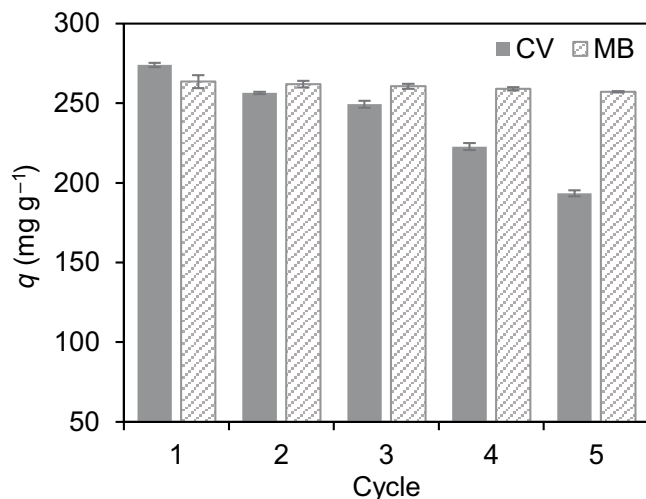
Fig. 6. Results of the reusability study of the MA-MOPH biosorbent.

Carboxyl group:

$$MA\text{-}MOPH - COOH + Dye - N^+(CH_3)_2 Cl^-$$
$$\rightarrow MA\text{-}MOPH - COO^- N^+(CH_3)_2 - Dye + H^+Cl^-$$

Hydroxyl group:

$$MA\text{-}MOPH - OH + Dye - N^+(CH_3)_2 Cl^-$$
$$\rightarrow MA\text{-}MOPH - O^- N^+(CH_3)_2 - Dye + H^+Cl^-$$

Moreover, the possible interaction between biosorbent and cationic dyes might be ascribed to hydrogen bonding between the H atom in carboxyl and hydroxyl groups of MA-MOPH and the N atom in the cationic dye molecules. An interaction was also probably formed through ion-dipole forces between partially negative charges on the O atom in carbonyl groups of MA-MOPH and positive charges in the CV and MB molecules [9,47].

4. Conclusion

A highly efficient lignocellulose biosorbent was prepared by chemically modifying *Moringa oleifera* pod husk biomass with maleic anhydride in a simple approach. The presence of carboxyl functional groups on the modified biosorbent promoted the adsorption of crystal violet and methylene blue in both a single and a binary dye system. Adsorption temperature hardly affected the adsorption of crystal violet and methylene blue on the modified biosorbent and the thermodynamic study indicated that the adsorption processes of both dyes were spontaneous and endothermic. In both dye systems, crystal violet and methylene blue were adsorbed on the modified biosorbent within 5 min. The adsorption of crystal violet and methylene blue in both systems was well fitted with the pseudo-second-order kinetics and Langmuir isotherm models. The model fitting implied that electrostatic adsorption was the dominant mechanism and that crystal violet and methylene blue adsorbed on the modified biosorbent in a monolayer. Moreover, by desorbing the modified biosorbent with 1.0 M CH$_3$COOH solution, adsorption capacity remained stable over five cycles of reuse. These results proved that carboxylate-modified *Moringa oleifera* pod husk was a practical and economic alternative biosorbent.

University for the financial support of Ms. Khoiria Nur Atika Putri (contract number: TEH-AC 030/2018). Mr. Thomas Coyne's kind assistance in English proofreading is also very much appreciated.

References

[1] W. McDonough, M. Braungart, Cradle to Cradle: Remaking the Way We Make Things, 1st ed., North Point Press, New York, 2002.

[2] K. Ruttarattanamongkol, A. Petrasch, Antimicrobial activities of *Moringa oleifera* seed and seed oil residue and oxidative stability of its cold pressed oil compared with extra virgin olive oil, Songklanakarin J. Sci. Technol., 37 (2015) 587–594.

[3] L. Gopalakrishnan, K. Doriya, D.S. Kumar, *Moringa oleifera*: a review on nutritive importance and its medicinal application, Food Sci. Hum. Wellness, 5 (2016) 49–56.

[4] N. Lehman, R. Phengthai, W. Chinpa, Effect of *Moringa oleifera* pod husk fibers on the properties of gelatin-based biocomposite, J. Polym. Environ., 26 (2018) 1405–1414.

[5] R.A. Wuana, R. Sha'Ato, S. Iorhen, Preparation, characterization, and evaluation of *Moringa oleifera* pod husk adsorbents for aqueous phase removal of norfloxacin, Desal. Water Treat., 57 (2016) 11904–11916.

[6] A. Keereerak, W. Chinpa, A potential biosorbent from *Moringa oleifera* pod husk for crystal violet adsorption: kinetics, isotherms, thermodynamic and desorption studies, ScienceAsia, 46 (2020) 186–194.

[7] F.A. Pavan, E.S. Camacho, E.C. Lima, G.L. Dotto, V.T.A. Branco, S.L.P. Dias, Formosa papaya seed powder (FPSP): preparation, characterization and application as an alternative adsorbent for the removal of crystal violet from aqueous phase, J. Environ. Chem. Eng., 2 (2014) 230–238.

[8] R. Lafi, N. Hamdi, A. Hafiane, Study of the performance of Esparto grass fibers as adsorbent of dyes from aqueous solutions, Desal. Water Treat., 56 (2015) 722–735.

[9] K.N.A. Putri, A. Keereerak, W. Chinpa, Novel cellulose-based biosorbent from lemongrass leaf combined with cellulose acetate for adsorption of crystal violet, Int. J. Biol. Macromol., 156 (2020) 762–772.

[10] A.P. Vieira, S.A.A. Santana, C.W.B. Bezerra, H.A.S. Silva, J.C.P. Melo, E.C.S. Filho, C. Airoldi, Copper sorption from aqueous solutions and sugar cane spirits by chemically modified babassu coconut (*Orbignya speciosa*) mesocarp, Chem. Eng. J., 161 (2010) 99–105.

[11] J. Yu, R. Chi, Z. He, Y. Qi, Adsorption performances of cationic dyes from aqueous solution on pyromellitic dianhydride modified sugarcane bagasse, Sep. Sci. Technol., 46 (2011) 452–459.

[12] Y. Zhou, Q. Jin, X. Hu, Q. Zhang, T. Ma, Heavy metal ions and organic dyes removal from water by cellulose modified with maleic anhydride, J. Mater. Sci., 47 (2012) 5019–5029.

[13] Y. Zhou, Y. Min, H. Qiao, Q. Huang, E. Wang, T. Ma, Improved removal of malachite green from aqueous solution using chemically modified cellulose by anhydride, Int. J. Biol. Macromol., 74 (2015) 271–277.

[14] H. Qiao, Y. Zhou, F. Yu, E. Wang, Y. Min, Q. Huang, L. Pang, T. Ma, Effective removal of cationic dyes using carboxylate-functionalized cellulose nanocrystals, Chemosphere, 141 (2015) 297–303.

[15] M. Ge, M. Du, L. Zheng, B. Wang, X. Zhou, Z. Jia, G. Hu, S.M. Jahangir Alam, A maleic anhydride grafted sugarcane bagasse adsorbent and its performance on the removal of methylene blue from related wastewater, Mater. Chem. Phys., 192 (2017) 147–155.

[16] X. Wen, C. Yan, N. Sun, T. Luo, S. Zhou, W. Luo, A biomass cationic adsorbent prepared from corn stalk: low-cost material and high adsorption capacity, J. Polym. Environ., 26 (2018) 1642–1651.

[17] S. Tangtubtim, S. Saikrasun, Effective removals of copper(II) and lead(II) cations from aqueous solutions by

[18] Y. Tang, T. Lin, C. Jiang, Y. Zhao, S. Ai, Renewable adsorbents from carboxylate-modified agro-forestry residues for efficient removal of methylene blue dye, J. Phys. Chem. Solids, 149 (2021) 109811, doi: 10.1016/j.jpcs.2020.109811.

[19] L. Segal, J.J. Creely, A.E. Martin, C.M. Conrad, An empirical method for estimating the degree of crystallinity of native cellulose using the X-ray diffractometer, Text Res. J., 29 (1959) 786–794.

[20] Y.F. Jia, B. Xiao, K.M. Thomas, Adsorption of metal ions on nitrogen surface functional groups in activated carbons, Langmuir, 18 (2002) 470–478.

[21] J.X. Yu, X.L. Cai, L.Y. Feng, W.L. Xiong, J. Zhu, Y.L. Xu, Y.F. Zhang, R.A. Chi, Synergistic and competitive adsorption of cationic and anionic dyes on polymer modified yeast prepared at room temperature, J. Taiwan Inst. Chem. Eng., 57 (2015) 98–103.

[22] Y. Pan, X. Shi, P. Cai, T. Guo, Z. Tong, H. Xiao, Dye removal from single and binary systems using gel-like bioadsorbent based on functional-modified cellulose, Cellulose, 25 (2018) 2559–2575.

[23] H.P.S.A. Khalil, H. Ismail, H.D. Rozman, M.N. Ahmad, The effect of acetylation on interfacial shear strength between plant fibres and various matrices, Eur. Polym. J., 37 (2001) 1037–1045.

[24] A. Alemdar, M. Sain, Isolation and characterization of nanofibers from agricultural residues – wheat straw and soy hulls, Bioresour. Technol., 99 (2008) 1664–1671.

[25] H. Kargarzadeh, I. Ahmad, I. Abdullah, A. Dufresne, S.Y. Zainudin, R.M. Sheltami, Effects of hydrolysis conditions on the morphology, crystallinity, and thermal stability of cellulose nanocrystals extracted from kenaf bast fibers, Cellulose, 19 (2012) 855–866.

[26] K. Obi Reddy, C. Uma Maheswari, M. Shukla, J.I. Song, A. Varada Rajulu, Tensile and structural characterization of alkali treated Borassus fruit fine fibers, Composites, Part B, 44 (2013) 433–438.

[27] G.Z. Kyzas, N.K. Lazaridis, A.C. Mitropoulos, Removal of dyes from aqueous solutions with untreated coffee residues as potential low-cost adsorbents: equilibrium, reuse and thermodynamic approach, Chem. Eng. J., 189–190 (2012) 148–159.

[28] L.S. Silva, J.O. Carvalho, R.D.S. Bezerra, M.S. Silva, F.J.L. Ferreira, J.A. Osajima, E.C. da Silva Filho, Potential of cellulose functionalized with carboxylic acid as biosorbent for the removal of cationic dyes in aqueous solution, Molecules, 23 (2018) 743, doi: 10.3390/molecules23040743.

[29] J. Liu, F. Chen, C. Li, L. Lu, C. Hu, Y. Wei, P. Raymer, Q. Huang, Characterization and utilization of industrial microbial waste as novel adsorbent to remove single and mixed dyes from water, J. Cleaner Prod., 208 (2019) 552–562.

[30] A. Aichour, H. Zaghouane-Boudiaf, Single and competitive adsorption studies of two cationic dyes from aqueous mediums onto cellulose-based modified citrus peels/calcium alginate composite, Int. J. Biol. Macromol., 154 (2020) 1227–1236.

[31] M.T. Nakhjiri, G.B. Marandi, M. Kurdtabar, Poly(AA-*co*-VPA) hydrogel cross-linked with *N*-maleyl chitosan as dye adsorbent: isotherms, kinetics and thermodynamic investigation, Int. J. Biol. Macromol., 117 (2018) 152–166.

[32] K.N.A. Putri, S. Kaewpichai, A. Keereerak, W. Chinpa, Facile green preparation of lignocellulosic biosorbent from lemongrass leaf for cationic dye adsorption, J. Polym. Environ., 29 (2021) 1681–1693.

[33] S. Lagergren, About the theory of so-called adsorption of soluble substances, Kungliga Svenska Vetenskapsakademiens, Handlingar, Band, 24 (1898) 1–39.

[34] Y.S. Ho, G. Mckay, Pseudo-second-order model for sorption processes, Process Biochem., 34 (1999) 451–465.

[35] S.J. Allen, Q. Gan, R. Matthews, P.A. Johnson, Kinetic modeling of the adsorption of basic dyes by kudzu, J. Colloid Interface Sci., 286 (2005) 101–109.

[36] S. Lapwanita, T. Sooksimuang, T. Trakulsujaritchok, Adsorptive removal of cationic methylene blue dye by kappa-carrageenan/

poly(glycidyl methacrylate) hydrogel beads: preparation and characterization, J. Environ. Chem. Eng., 6 (2018) 6221–6230.

[37] S. Rangabhashiyam, N. Anu, M.S. Giri Nandagopal, N. Selvaraju, Relevance of isotherm models in biosorption of pollutants by agricultural by-products, J. Environ. Chem. Eng., 2 (2014) 398–414.

[38] I. Langmuir, The adsorption of gases on plane surfaces of glass, mica, and platinum, J. Am. Chem. Soc., 40 (1918) 1361–1403.

[39] H.M.F. Freundlich, Over the adsorption in solution, J. Phys. Chem., 57 (1906) 385–470.

[40] S. Bentahar, A. Dbik, M.E. Khomri, N.E. Messaoudi, A. Lacherai, Adsorption of methylene blue, crystal violet and Congo red from binary and ternary systems with natural clay: kinetic, isotherm, and thermodynamic, J. Environ. Chem. Eng., 5 (2017) 5921–5932.

[41] E. Sharifpour, H. Haddadi, M Ghaedi, Optimization of simultaneous ultrasound assisted toxic dyes adsorption conditions from single and multi-components using central composite design: application of derivative spectrophotometry and evaluation of the kinetics and isotherms, Ultrason. Sonochem., 36 (2017) 236–245.

[42] T. Benhalima, H. Ferfera-Harrar, D. Lerari, Optimization of carboxymethyl cellulose hydrogels beads generated by an anionic surfactant micelle templating for cationic dye uptake: swelling, sorption and reusability studies, Int. J. Biol. Macromol., 105 (2017) 1025–1042.

[43] Y. Tang, T. Lin, S. Ai, Y. Li, R. Zhou, Y. Peng, Super and selective adsorption of cationic dyes using carboxylate-modified lignosulfonate by environmentally friendly solvent-free esterification, Int. J. Biol. Macromol., 159 (2020) 98–107.

[44] X.-F. Sun, S.-G. Wang, X.-W. Liu, W.-X. Gong, N. Bao, B.-Y. Gao, Competitive biosorption of zinc(II) and cobalt(II) in single- and binary-metal systems by aerobic granules, J. Colloid Interface Sci., 324 (2008) 1–8.

[45] Y. Li, H. Xiao, Y. Pan, M. Zhang, Y. Jin, Thermal and pH dual-responsive cellulose microfilament spheres for dyeremoval in single and binary systems, J. Hazard. Mater., 377 (2019) 88–97.

[46] M.A.P. Cechinel, S.M.A.G. Ulson De Souza, A.A. Ulson de Souza, Study of lead(II) adsorption onto activated carbon originating from cow bone, J. Cleaner Prod., 65 (2014) 342–349.

[47] T. Marhaendrajana, R. Kurnia, D. Irfana, D. Abdassah, D. Wahyuningrum, Study to improve an amphoteric sulfonate alkyl ester surfactant by mixing with nonionic surfactant to reduce brine-waxy oil interfacial tension and to increase oil recovery in sandstone reservoir: T-KS field, Indonesia, J. Pet. Explor. Prod. Technol., 9 (2019) 675–683.